



CHALMERS
UNIVERSITY OF TECHNOLOGY



Chemical Looping Combustion of Biomass

Using pine sawdust as fuel and ilmenite as oxygen carrier

Master's Thesis in the Master's Programmes:
Innovative and Sustainable Chemical Engineering
Sustainable Energy Systems

EMIL LILLIEBLAD
ANNA MÅRTENSSON

Department of Chemistry and Chemical Engineering
Division of Energy and Materials
CHALMERS UNIVERSITY OF TECHNOLOGY
Gothenburg, Sweden 2019

MASTER'S THESIS 2019

Chemical Looping Combustion of Biomass

Using pine sawdust as fuel and ilmenite as oxygen carrier

EMIL LILLIEBLAD
ANNA MÅRTENSSON



CHALMERS
UNIVERSITY OF TECHNOLOGY

Supervisor, Chalmers: Henrik Leion
Supervisor, Monash University: Sankar Bhattacharya

Department of Chemistry and Chemical Engineering
Division of Energy and Materials
CHALMERS UNIVERSITY OF TECHNOLOGY
Gothenburg, Sweden 2019

Chemical Looping Combustion of Biomass
Using pine sawdust as fuel and ilmenite as oxygen carrier

EMIL LILLIEBLAD
ANNA MÅRTENSSON

© EMIL LILLIEBLAD & ANNA MÅRTENSSON, 2019.

Master's Thesis 2019

Department of Chemistry and Chemical Engineering
Division of Energy and Materials
Chalmers University of Technology
SE-412 96 Gothenburg
Telephone +46 (0)31 772 1000

Cover:
Photo of the pine sawdust used as fuel and ilmenite used as oxygen carrier in the thesis.

Chalmers digitaltryck
Gothenburg, Sweden 2019

Chemical Looping Combustion of Biomass
Using pine sawdust as fuel and ilmenite as oxygen carrier
EMIL LILLIEBLAD & ANNA MÅRTENSSON
Department of Chemistry and Chemical Engineering
Division of Energy and Materials
Chalmers University of Technology

Abstract

Chemical Looping Combustion, CLC, is a novel technological combustion process used to enable Carbon Capture and Storage, CCS. It is enabled by using oxygen carrier to support the combustion process with oxygen instead of directly feeding air into the chamber resulting in avoidance of nitrogen in the flue gas, which makes the separation of carbon dioxide more convenient. In this thesis, biomass is evaluated as fuel in a CLC experimental process with mainly ilmenite as oxygen carrier. Biomass, which is used in this study, consist of a high fraction of volatiles compared to other fuels. Hence, the conversion of these volatiles is the focus in this thesis. More specifically, using a single or double bed setup, the effect of residence time and the ratio between the amount of fuel and oxygen carrier is analyzed. Finally, another oxygen carrier, hematite, was used as well to be able to compare the results with ilmenite. The results are measured in terms of conversion of CO and the total oxygen demand.

The experiments were carried out in a smaller quartz reactor which function as a batch reactor where the oxidation and reduction phases alternate. The reactor has two different beds on which the oxygen carrier can be placed. The amount of oxygen carrier ranged from 20 to 60 g and the amount of biomass ranged from 0.075 to 0.225 g. The temperature of the reactor was kept at around 950 °C and the total flow rate at around two times the minimum fluidization velocity. The gas introduced into the system was a mixture of either N₂ and CO₂ or air depending on if oxidizing the oxygen carrier or gasifying the fuel.

The first finding was from identifying a particular particle size and pruge flow rate which suits the system best. This was found to be 1700-2000 μm and 0.9 L/min respectively. Further, one conclusion of this thesis is that using the bed which is located up-streams from the fuel inlet is beneficial as the residence time between the volatiles and the oxygen carrier grows longer. A higher conversion of CO and lower oxygen demand was observed with a longer residence time, hence a longer residence time is favorable. It was further found that an increase of amount of fuel compared to the amount of oxygen carrier in the system showed better results. Finally, comparing the results to another oxygen carrier, hematite in this case, was found to show the same trends as for ilmenite. However, the results for hematite were significantly better as the conversion of CO was higher and the oxygen demand lower.

Keywords: CLC, Oxygen Carrier, Biomass, Pine sawdust, Ilmenite, Hematite

Acknowledgements

We would like to begin by thanking Prof. Sankar Bhattacharya and our examiner Dr. Henrik Leion for the opportunity to conduct this master in Melbourne, Australia. We would also like to give our gratitude to Prof. Bhattacharya for his warm welcome, support and work to include us in his group.

Further, we would like to express our thanks to everyone at Chemical Engineering and their warm welcome to include us in their department with both great advise and pleasant conversations.

Finally, we would like to express our greatest gratitude to PhD-student Mr. Imtenan Sayeed who has worked tirelessly to guide us through our challenges regardless of his own high workload for which we cannot thank him enough.

Emil Lillieblad & Anna Mårtensson, Melbourne, June 2019

CONTENTS

Abbreviations	ix
Nomenclature	xi
List of Figures	xi
List of Tables	xii
1 Introduction	1
1.1 Background	1
1.2 Problem Formulation	4
1.3 Aim	4
1.4 Delimitations	5
2 Theory	6
2.1 Chemical Looping Combustion	6
2.1.1 Direct solid fuel conversion processes	6
2.1.2 Fluidizing beds	7
2.1.3 Reactor configurations	8
2.2 Oxygen Carrier	8
2.3 Fuel	11
2.4 Calculation of Results	11
2.4.1 Minimum fluidization velocity	12
2.4.2 Conversion of CO	12
2.4.3 Oxygen demand	13
2.5 Analysis	13
2.5.1 Thermogravimetric analysis	13
2.5.2 Infrared spectroscopy	13
2.5.3 Thermal conductivity	14
2.5.4 Temperature programmed reduction	14
3 Methodology	15
3.1 Experimental Setup	15
3.2 Preparation of Experiments	17
3.2.1 Fuel	17
3.2.2 Oxygen carrier	18
3.3 Conduction of Experiments	18

CONTENTS

3.3.1	Description of an experimental cycle	19
3.3.2	Values of constant parameters	19
3.3.3	Gas composition	20
3.3.4	Optimization of experimental parameters	20
3.3.4.1	Particle size and purge flow rate	21
3.3.4.2	Dual or single fluidizing bed	21
3.3.4.3	Residence time	21
3.3.4.4	Fuel/OC ratio	22
3.3.5	Residence time using hematite	22
3.4	Other Setups and Methods used	22
3.4.1	Metallic reactor	22
3.4.2	Temperature programmed reduction	23
4	Results and Discussion	25
4.1	Gas Composition	25
4.2	Optimization of Experimental Parameters	26
4.2.1	Particle size and purge flow rate	27
4.2.2	Dual or single fluidizing bed	28
4.2.3	Residence time	29
4.2.4	Fuel/OC ratio	31
4.3	Residence Time using Hematite	33
4.4	Other Setups and Methods used	35
4.4.1	Metallic reactor	36
4.4.2	Temperature programmed reduction	36
5	Conclusion	37
5.1	Future Work	38
	Bibliography	38
A	Analysis of fuel	I

ABBREVIATIONS

Al_2O_3	Aluminum Oxide
C	Carbon
CCS	Carbon Capture and Storage
CCU	Carbon Capture and Utilization
CFB	Circulating Fluidized Bed
CLC	Chemical Looping Combustion
CLOU	Chemical Looping with Oxygen Uncoupling
CH_4	Methane
CO	Carbon monoxide
CO_2	Carbon dioxide
Cu	Copper
CuO	Tenorite
Fe	Iron
Fe_2O_3	Hematite
Fe_3O_4	Magnetite
$\text{Fe}_2\text{Ti}_3\text{O}_9$	Pseudorutile/Oxidized form of Ilmenite
FeTiO_3	Ilmenite
FeTiO_5	Pseudo-brookite/Active phase of Ilmenite
H_2O	Hydrogen dioxide/water/steam
H_2	Hydrogen gas
iG-CLC	Insitu Gasi cation Chemical Looping Combustion
IR	Infrared
kW_{th}	Kilowatt thermal
Me	Metal in oxygen carrier
MeO_x	Oxidized oxygen carrier
MeO_y	Reduced oxygen carrier
Mn	Manganese
μm	Micrometer
Ni	Nickel
O_2	Oxygen gas
OC	Oxygen Carrier

CONTENTS

ppm	parts per million
S	Sulfur
SiO ₂	Silicon dioxide
TGA	Thermogravimetric Analysis
TiO ₂	Rutile/Titanium dioxide
TPR	Temperature Programmed Reduction
vol%	Volumetric percentage
wt%	Weight percentage

NOMENCLATURE

Ar	Archimedes dimensionless number
d_p	Particle size of the oxygen carrier
DTG	Weight loss per minute
F_{out}	Total molar flow rate in the outlet
g	The gravity constant
M_C	Molar mass of carbon
M_O	Molar mass of oxygen
$m_{CO;out}$	Mass of CO after the reactor
$m_{CO;tot}$	Mass of CO generated by the fuel
m_{fuel}	Amount of biomass
	Viscosity of air
μ_{fuel}	Constant representing the amount of oxygen needed to burn the fuel
OD	Oxygen demand
T	Total oxygen demand
U_{mf}	Minimum fluidization velocity
p	Pressure
R	Ideal gas constant
Re_{mf}	Reynolds dimensionless number
	Density of air
ρ_p	Density of the oxygen carrier
t	Time for one reduction cycle
T	Temperature
TG	Weight loss
V_{out}	Volumetric flow rate
X_{CO}	Conversion of CO
$X_{H_2;out}$	Fraction of H_2 in the outlet gas
$X_{CH_4;out}$	Fraction of CH_4 in the outlet gas
$X_{CO;out}$	Fraction of CO in the outlet gas

LIST OF FIGURES

1.1	The three different possibilities for carbon capture.	3
1.2	An overview of how a CLC process functions.	4
3.1	The quartz reactor in the experimental setup.	16
3.2	The entire setup of the process.	17
3.3	The metallic reactor which was used in initial experiments.	23
3.4	The smaller cylinder which slides into the larger part of the reactor with a bed attached to it through cement.	23
3.5	The setup in the TPR experiments.	24
4.1	A graph of the gas composition over time for biomass.	26
4.2	The composition of the different gases in the outlet during a reduction cycle.	27
4.3	The oxygen demand over time for a reduction cycle.	27
4.4	The conversion of CO with increasing amount of oxygen carrier in top bed.	29
4.5	The total oxygen demand with increasing amount of oxygen carrier in top bed.	29
4.6	The conversion of CO with increasing residence time.	30
4.7	The total oxygen demand with increasing residence time.	31
4.8	The conversion of CO with increasing fuel/OC ratio.	32
4.9	The total oxygen demand with increasing fuel/OC ratio.	32
4.10	The conversion of CO for hematite with increasing residence time.	33
4.11	The total oxygen demand for hematite with increasing residence time.	34
4.12	The conversion of CO for both ilmenite and hematite with increasing residence time.	35
4.13	The total oxygen demand for both ilmenite and hematite with increasing residence time.	35
A.1	Analysis of pine sawdust in terms of weight loss (TG) and weight loss per minute (DTG) of the sample over time with changing temperature.	I

LIST OF TABLES

3.1	Dry basis percentage of constituents in solid fuel.	18
3.2	Values of the parameters kept constant throughout all experiments during different parts of the experimental cycle.	20
3.3	The different configurations for analyzing dual or single bed options.	21
3.4	The different configurations for analyzing residence time.	22
3.5	The different fuel/OC ratios with corresponding amount of fuel.	22

1

INTRODUCTION

The introductory chapter aims to introduce the reader into the topic of carbon capture and storage and chemical looping combustion. It aims to provide a basis of understanding before focusing on the topic in more detail in chapter 2. Further, this chapter will explain the challenges of this field as well as the aim and delimitations of this thesis.

1.1 Background

According to the IPCC it is with at least a 95 % certainty that humans are the main cause of global warming [1]. To limit the risk and impact of climate change the Paris Agreement was constructed and has been signed by several nations in a united force to hinder global warming which is one of the agreement's main objectives [2]. More specifically, it is written with the agreement of holding ... the increase in the global average temperature to well below 2°C above pre-industrial levels ... [2]. Before the industrial age the concentration of CO₂ in the air was about 280 ppm [3]. Since then, the concentration has increased dramatically and has today reached levels of about 406 ppm as measured in October 2018 which corresponds to an increase by 45 % [4]. The concentration of CO₂ in the air and the increase of the global average temperature is connected, however to what degree is a bit unclear [5]. There are different scenarios of ranges connecting CO₂ to the increase in temperature which was summarized from multiple sources [5]. In some of these scenarios the concentration of greenhouse gases in the atmosphere need to be decreased as soon as 2060 to limit the temperature increase and hence uphold the Paris Agreement. To achieve a decrease in concentration of the greenhouse gases there is reliance on certain technologies, such as for example biomass energy with carbon capture and storage [5].

Carbon capture and storage (CCS), as well as carbon capture and utilization (CCU) are two methods to decrease the emissions from both fossil fuels and the usage of biomass [6]. CCS is based on capturing the CO₂ which otherwise would be emitted into the air and store it deep underground, for example in depleted oil and gas fields, to avoid its affect on the climate [7]. CCU is a method which instead uses the captured CO₂ to produce products such as for example plastics [8]. However, it should be noted that CCU's potential is a topic of discussion in terms of how much impact CCU can have on mitigating the growing concentration of CO₂ in the atmosphere, CCS on the other hand is considered to have a higher potential due to scale and how far the research has gone [9]. CCS and CCU can produce negative emissions

1. Introduction

when using biomass as the source of the CO_2 captured [6]. The emissions become negative since the net emissions of CO_2 when using biomass as fuel, is zero. The net emissions are zero since the biomass used has grown through using CO_2 from the atmosphere, hence releasing the CO_2 back into the atmosphere which does not contribute to further emissions [10].

Since the flue gases in regular combustion has a fraction of 3-15 % CO_2 needs to be separated from all other gases for effective storage, there are a number of different methods to be able to capture CO_2 and hence use CCS or CCU, these are shown in figure 1.1 [11] [12]. Firstly, if fuel has gone through combustion, the CO_2 in the flue gases can be chemically absorbed in order to capture it which is called flue gas separation or post-combustion capture. Secondly, in the method of pre-combustion capture, gasification of the fuel takes place which through a series of further process steps leads to the CO_2 being separated creating a hydrogen-rich fuel gas to use as fuel instead [12]. Finally, the combustion could instead be carried out in pure or enriched oxygen, called oxyfuel combustion, which would lead to the flue gases primarily existing of only CO_2 and H_2O from which the steam is easily removed through condensation [11].

Figure 1.1: The three different possibilities for carbon capture.

One technique for carbon capture within oxyfuel combustion is Chemical Looping Combustion (CLC) where fuel is burnt in an environment with CO_2 , steam and oxygen which is introduced through an oxygen carrier (OC). The OC carries oxygen from an environment in air, through which the oxygen is brought into the fuel combustion [13]. The lack of other gases in the environment leads to the exhaust mainly being composed of steam and CO_2 hence a process which works well for CCS or CCU as the steam can simply be condensed. CLC is shown in figure 1.2 which describe how the fuel-reactor is supplied with oxygen through the oxygen carrier which is transferred between two reactors. The oxygen carrier, when oxidized, is denoted in this figure by MeO_x in which Me signifies some metal which carries the oxygen while x and y corresponds to the number of oxygen atoms bonded to the metal in which x is always larger than y . When the oxygen carrier has been oxidized in the air-reactor, it is moved to the fuel-reactor in which the oxygen is used for fuel combustion. Part of the fuel-gases can be recirculated into the fuel-reactor to be used as a oxidizing gas [14].

Figure 1.2: An overview of how a CLC process functions.

1.2 Problem Formulation

As described earlier, using biomass as fuel in carbon capture processes, such as CLC, lead to negative emissions of CO₂. However, biomass has not been the main focus of CLC research within solid fuels, coal has been instead [15]. Compared to coal, biomass has a significantly higher degree of volatile matter which is released during the CLC process [16] [17] [18]. Hence, using biomass instead of coal in CLC leads to different requirements upon the process. To be able to prepare to use CLC with biomass commercially, more research is needed especially with regards to the significantly higher amount of volatiles that are released while using biomass.

1.3 Aim

The aim of the thesis is to contribute with additional research within the area of using biomass as fuel in CLC focusing on the volatiles released. Further, the aim is to analyze operation parameters for a bench scale reactor.

More specifically the following objectives to be achieved in this thesis are:

- ^ Study which particle size and purge gas flow which is optimal for usage in the experimental setup used.
- ^ Analyze the results when using single or double fluidized beds as well as where it is located relative to where the fuel is fed.
- ^ Analyze how residence time affects the results through changing the amount of oxygen carrier.
- ^ Study the ratio between fuel and oxygen carrier and how it affects the results.
- ^ Compare results to another oxygen carrier to analyze if the same trends are present when studying residence time and how the two compare to each other.

1.4 Delimitations

Due to time limitation, the master thesis will focus only on one biomass fuel and two oxygen carriers. The biomass fuel used in this research is pine sawdust and the oxygen carriers are ilmenite and hematite. However, the primary focus will be on ilmenite. The thesis is restricted to only analysis on a bench scale reactor. Hence, the findings may not be applicable on reactors of different size.

2

THEORY

This chapter will focus on the theoretical background to CLC, oxygen carriers, fuel, how the results were calculated and methods for analysis. It aims to give the reader a thorough understanding of this field of research and the choices that have been made during this thesis work.

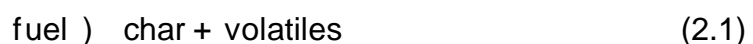
2.1 Chemical Looping Combustion

This section focus on explaining CLC in more detail including conversion processes that the fuel and oxygen carrier undergoes, how fluidization work and different reactor configurations used for CLC.

For solid fuels, such as biomass, there are two major types of chemical looping processes, one is syngas-CLC and the other is direct solid fuel CLC. In this thesis, direct solid fuel CLC will be in focus and is further described in the following section (2.1.1). To give a brief explanation of syngas-CLC, three central steps are carried out. First, the fuel is pyrolyzed into char and volatile gas. Secondly, the char is gasified into syngas and finally both the volatile gas and syngas reacts with the oxygen carrier to produce CO and H_2O . Hence, the pyrolysis and gasification is carried out before the chemical looping process which the volatile gas and syngas then enters. Further, syngas is defined as being a mixture of H_2 and CO . [19]

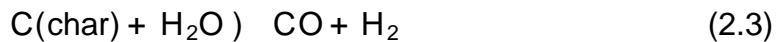
2.1.1 Direct solid fuel conversion processes

In direct solid fuel CLC, the fuel is fed directly into the fuel reactor, a series of different mechanisms are taking place. The first two processes are drying and devolatilization. Devolatilization is the process when the fuel is generating volatiles and char, described by equation 2.1. [19] The volatiles generated by the biomass is mainly consisting of CO , H_2 and CH_4 [20].

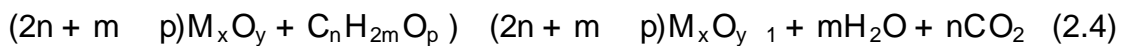


Depending on choice of oxygen carrier and temperature there are mainly two different char conversion processes; iG-CLC (insitu gasification CLC) and CLOU (Chemical Looping with Oxygen Uncoupling) [21]. The solid-solid reaction between the char particle and the oxygen carrier is not likely to occur at an appreciable rate when fluidizing the oxygen carrier and fuel together [22]. Hence, these two processes are two different ways to increase the speed of the reaction.

For iG-CLC the remaining char is not directly oxidized by the oxygen carrier, but involves an intermediate gasification step. The char is gasified by the fluidizing gas consisting of CO_2 and/or H_2O , described by equation 2.2 and 2.3 [19][21]. The gasification step is slow compared to the oxidation of the syngas and the gaseous hydrocarbons and is the rate limiting step. [19]



The volatiles and the produced syngas is then oxidized by the oxygen carrier in three different ways. The CO is converted into CO_2 , the H_2 to H_2O and finally the gaseous hydrocarbon content is oxidized according to equation 2.4 [23] [19].



In contrary, for CLOU it is the oxygen that is the gaseous phase to enable a reaction between the oxygen and the char. The oxygen becomes gaseous because the oxygen carriers used, to achieve the CLOU conversion process, spontaneously decompose at higher temperature into its reduced form and release oxygen gas in the fuel reactor. The released oxygen is then reacting with the char and the volatiles. The advantage with this process is that the slow gasification step is not necessary. The drawbacks are however that the oxygen carrier is relatively expensive compared to the Fe-based oxygen carriers often used in iG-CLC. Further challenges with oxygen carriers used in CLOU are that some of them, copper for example, is mechanically unstable and has a low melting point. iG-CLC has been chosen in this master thesis due to the oxygen carriers that can be studied with this method of which more information will be provided in section 2.2. [24]

2.1.2 Fluidizing beds

A fluidizing bed is when solid particles present on a perforated bed is lifted and agitated by a rising stream of fluid, the fluid can be both gas or liquid. For the fluidization to occur the velocity has to be high enough so the friction force acting on the particles from the rising fluid is higher than the gravitational force of the particle. The velocity needed to exactly counteract the gravitational force is called the minimum fluidization velocity, how to calculate it is described in section 2.4.1. When the velocity in a solid-liquid system increases above the minimum fluidization velocity it results in an expanding bed and an increased bed height. A solid-gas system behaves quite differently. Instead of a smooth expansion it results in bubbling, channeling of the gas and even slugging of particles. [25]

Since the bed is constantly mixing and moving it is good for different combustion processes because it results in rapid heat and mass transfer. It effectively evens out temperature and concentrations in the bed. The pressure drop over a fluidized

bed is usually very low. A widely spread technology is to use this phenomena in a CFB-boiler in which CFB is an abbreviation of circulating fluidized bed. The advantages of using a CFB-boiler is its wide flexibility using different fuels, high combustion efficiency and low emissions.

2.1.3 Reactor configurations

There are several different types of reactor configurations that can be used for a CLC system. A commonly used reactor configuration is using two interconnected fluidizing bed reactors where the oxygen carrier is transported between them, see figure 1.2. The advantages with this kind of system is many; high carbon conversion, good contact between gas and solids, even temperature and small pressure drop. However, the system that circulate the oxygen carrier in the system is both energy intensive and complex.[26] To address the issue of the slow gasification step described in section 2.1.1 configurations with multiple fuel reactors can be used to increase the total residence time of the char particles in the system resulting in higher conversion of the fuel. This type of configurations consists of multiple fluidizing beds in series. It comes with a big investment and a complex design so it has mainly only been evaluated on a modelling scale.[27][28] In this thesis a fuel reactor with two fluidizing beds at different levels was used in order to increase the conversion of volatiles by increasing the contact time between the volatiles and the oxygen carrier.

As an alternative to the fluidizing bed reactors different fixed bed configurations have been studied. One fixed bed alternative is to just have a fixed bed of oxygen carrier and alternate a reductive fuel flow and an oxidizing air flow. To have a continuous process, two or more reactors operating simultaneously but with different flows need to be used, one in which oxidizing gas is always used and the other which is always reduced by fuel. [26] Another fixed bed alternative is to use a rotary reactor design. The concept of the process is to rotate a fixed bed of oxygen carrier continuously through four different sections: fuel, air and two purge sections which separates the air from the fuel. The fixed bed is rotated above the gas and fuel flow streams which move upwards through the bed of oxygen carrier. [29] A drawback with these fixed bed configurations is that the fuel either needs to be gaseous or be converted into gaseous form (gasified to syngas).

2.2 Oxygen Carrier

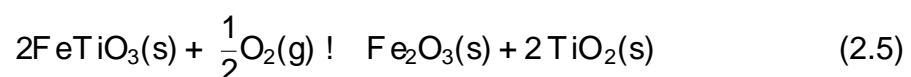
The oxygen carrier, which supplies the fuel reactor in CLC with oxygen, is an important part of the system and has to have multiple characteristics to be able to function well. Firstly, the oxygen carrier needs to have a high reactivity for both the reduction and oxidation reactions, favourable thermodynamics when it comes to the fuel conversion and high enough oxygen transport capacity, or in other words how much oxygen the oxygen carrier is able to absorb and desorb. Further, a good oxygen carrier has resistance to attrition, has good fluidizing properties and very low carbon decomposition. At the same time, the oxygen carrier should be cost efficient and be environmentally friendly. [23]

Several elements are able to act as oxygen carriers and have different characteristics. Some examples that have favourable reductive and oxidative thermodynamic properties include copper (Cu), iron (Fe), manganese (Mn), and nickel (Ni) [30] [31]. Copper-based oxygen carriers, as mentioned earlier, has the disadvantage of being relatively in-stable mechanically and has a low melting point [24]. Further, manganese-based has the advantage of having high oxygen consumption and hence effective in that aspect. The only oxygen carrier which has a higher oxygen consumption is iron-based ones showing a higher regeneration of active sites where oxygen can adsorb at oxidation. Further, iron oxides occur naturally which lead to both a more economically, but also more environmentally, friendly alternative. [32] Finally, using nickel as an oxygen carrier is advantageous at high temperatures as thermal stability and reactivity, for reacting with syngas among others, is superior [33]. However, nickel is instead easily deactivated by sulfur [34] and is toxic. [31]

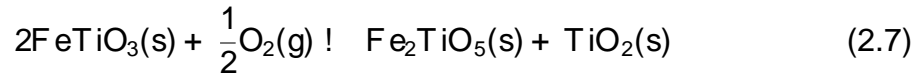
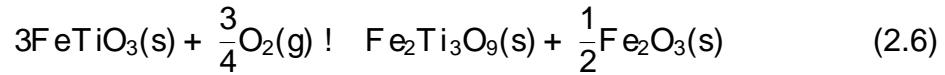
CLOU and iG-CLC were mentioned as two methods for solid-gas reactions in section 2.1. Using the CLOU method, the oxygen carriers need to release oxygen at certain temperatures. Examples of oxygen carriers that have the ability to release oxygen at temperatures at around 800 to 1000°C is CuO [35] and manganese oxide systems with other mixed oxides such as MnFe or MnSi-oxides [36]. For iG-CLC it is important that the oxygen carrier has high reactivity during both the reduction and oxidation cycle. Typical oxygen carriers for iG-CLC are for example nickel, iron and other manganese-based oxides. [37]

Further, oxygen carriers presented in literature are divided into two groups, synthetic materials and natural minerals. The synthetic materials are usually made of single metal oxides, combined or mixed metal oxides together with an inert support such as for example aluminum oxide, Al_2O_3 , and silicon dioxide, SiO_2 . The natural minerals are materials such as iron ore, ilmenite or waste materials from the steel industry. The advantage of using synthetic materials is because of the higher reactivity compared to natural minerals, however it is instead more expensive. During CLC, ash will blend with the oxygen carries decreasing its efficiency. Since ash and the oxygen carrier will be difficult to separate from each other, it is easier to discard the oxygen carrier together with the ash. Hence, cheaper types of oxygen carriers are sought after. [19]

The natural mineral ilmenite is an example of a relatively cheap oxygen carrier. Further, Australia exports 40 % of the world's ilmenite and hence is an important resource to further study which is why it has been chosen in this thesis [38]. Ilmenite mineral consist of ilmenite ($FeTiO_3$), hematite (Fe_2O_3) and impurities. Its oxidizing reactions is shown in equations 2.5, 2.6 and 2.7. Which of these reaction that occur depends on the temperature ranges of 500-750°C, 770-890°C and above 900°C respectively [39].



2. Theory

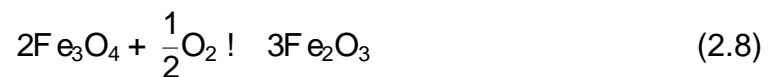


The active phases of Ilmenite, when used as an oxygen carrier, contain Fe_2TiO_5 , pseudo-brookite, and Fe_2O_3 [39] [40]. The temperature used for the experiments in this master thesis will lead to equation 2.7 primarily occurring. Hence, Fe_2TiO_5 will be the primary active phase and oxidized form of ilmenite. Ilmenite occurs as weathered sand or as rock ore depending on where it is mined out. [41] The chemical properties of the ilmenite can differ quite much so it is important to evaluate each sample individually.

Before using an oxygen carrier in the CLC process it is desirable to treat it in some manner to gain more stable results. For ilmenite, for example, both calcination and activation should be carried out. Research has been conducted which shows benefits with conducting this procedure on the oxygen carrier. Calcination is a process in which the oxygen carrier is heated up to high temperatures (for example 950°C) during a longer period of time [42]. The calcination increases the reaction rate of the oxygen carrier and oxidizes it to its most oxidized state. Further, activation of ilmenite has been found to be faster if the ilmenite has been calcinated before activation. [43]

The activation of ilmenite is reached through continuous alternating reducing and oxidizing cycles. How many cycles which are needed are, among other, dependent upon the length of the cycles. Literature has reported the cycles to be between 1-30 minutes while the number of cycles may range between 4-40. The oxygen carrier can be said to be activated when the conversion during reduction has stabilized and reaches the same percentage during several cycles. The benefits of activation include increase of conversion through higher reaction rates in both oxidation and reduction and significantly higher porosity. However, this also leads to the hardness to be significantly lower in activated ilmenite than fresh. [43]

Another iron-based natural ore used as oxygen carrier in this thesis is hematite. Hematite is mainly composed of Fe_2O_3 which is also its active phase and is considered to have a relatively low price and be environmentally friendly [44]. One reason for the low price is its large resources, for example in Australia 96 % of the iron ore export is hematite [45]. Further, hematite is very reactive in the beginning but quite quickly, over a few cycles, loses its high reactivity and will afterwards be at a lower, yet favorable, but more similar reactivity between the cycles. [46] For this reason hematite needs treatment before using it as well through both calcination but also through carrying out a couple of cycles to reach similarity in reactivity. Due to hematite's favorable qualities, relatively good reactivity and similarity to ilmenite in being iron-based it was chosen as an oxygen carrier to compare results with ilmenite. The oxidizing reaction of hematite is shown in equation 2.8 [47] in which Fe_3O_4 is magnetite, the reduced form of hematite [46] [48].



2.3 Fuel

There are several types of fuels which have been tested previously in literature, including both gaseous and solid fuels. Examples of gaseous fuels in prior CLC studies are natural gas and propane [31]. Using solid fuels in CLC has shown several differences in the demands on the process compared to using gaseous fuels. Solid fuels will create ash which will mix with the oxygen carrier and shorten the time available for usage. Further, the gasification of char is a relatively slow process which therefore increases the demands on the process to provide a long enough residence time. Finally, the fuel needs to be introduced into the CLC system in such a way that the volatiles released from the solid fuels have good contact with the fluidizing bed to ease the conversion. [15] The amount of char, volatiles and ash contents depend further on what type of solid fuel which is used. Examples of solid fuels are coal, coke and biomass.

Within coal there are several different kinds such as anthracite, bituminous and lignite which also differ between each other. For example, anthracite and lignite have a significantly higher ash content than bituminous at around 25 to 30%. The amount of volatile matter ranges between around 7 to 30 %, further showing the large difference different types of coals can have. [17]

Similarly, there are many types of biomass fuels with large differences between them. Based on an article analyzing ash content and volatile matter on 13 different biomasses some general aspects can be noted. The ash content is significantly lower, at most 10 %, and volatile matter, ranging between 70 to 85 %, is significantly higher in biomass compared to coal [18]. Due to the higher amount of volatiles present in biomass, the oxygen demand is higher as well [49]. Oxygen demand is a ratio between the amount of oxygen lacking to achieve complete combustion compared to the theoretical amount of oxygen needed which will be further presented in section 2.4.3 [50].

In this thesis pine sawdust will be used as biomass. The interest of pine and choice of it for this thesis is due to its presence in both Australia and Sweden. Australia's commercial forests comprises of 1 million acres of softwood trees of which most are pine trees [51]. In Sweden 39 % of the forest is pine [52], hence research of using pine as biomass in both these countries are of interest as there is plenty of it.

2.4 Calculation of Results

In this section it is presented how the results are calculated of which the analysis is based on. This includes calculations of minimum fluidization velocity, conversion of CO and the oxygen demand.

2.4.1 Minimum fluidization velocity

To predict the minimum fluidization velocity, which was described in section 2.1.2, there are more than a hundred different correlations. Most, on the other hand, are functions of Reynolds (Re_{mf}) and Archimedes (Ar) dimensionless numbers. Equation 2.9 shows how U_{mf} is connected to Re_{mf} . [53]

$$U_{mf} = \frac{Re_{mf}}{d_p} \quad (2.9)$$

In which μ is the viscosity of air, ρ_a is the density of air and d_p is the particle size of the oxygen carrier. Further, Re_{mf} and Ar can be calculated through using equation 2.10 and 2.11 respectively [54] [53].

$$Re_{mf} = (33.7^2 + 0.0408Ar)^{0.5} - 33.7 \quad (2.10)$$

$$Ar = \frac{g (\rho_p - \rho_a) d_p^3}{\mu^2} \quad (2.11)$$

In equation 2.11 g is 9.82 m/s^2 , or in other words the gravity constant, and ρ_p is the density of the oxygen carrier.

2.4.2 Conversion of CO

The volatiles, based on results presented in section 4.1 comprises to a high degree of carbon monoxide (CO). Further, ilmenite reacts quite ineffectively with CO which is why this thesis focuses more specifically on the conversion of CO [24]. The conversion of CO is a measurement of how much of the CO from the fuel which is converted in the process into CO_2 . The conversion of CO indicates how efficiently the system work as one of the goals is to analyze how the system can be as efficient as possible with regards to the low reactivity that ilmenite has with CO. To calculate the conversion of CO, the mass of CO after the reactor $m_{CO;out}$, is divided by the mass of CO which is produced through devolatilization of the fuel $m_{CO;tot}$ as shown in equation 2.12. Further, $m_{CO;out}$ is calculated by equation 2.13 while $m_{CO;tot}$ is calculated using the same equation but through the procedure described in section 3.3.3, without the presence of oxygen carrier.

$$X_{CO} = 1 - \frac{m_{CO;out}}{m_{CO;tot}} \quad (2.12)$$

$$m_{CO;out} = \frac{pM_C}{RT} \int_0^{Z_t} V_{out}(x_{CO;out}) dt \quad (2.13)$$

In equation 2.13, p is the pressure, M_C is the molar mass of carbon, R is the ideal gas constant, T is the temperature, V is the volumetric flow rate and $x_{CO;out}$ is the fraction of CO in the outlet gas.

2.4.3 Oxygen demand

The oxygen demand, OD , is described in terms of a ratio between the amount of oxygen lacking to achieve complete combustion against the theoretical amount of the oxygen needed [50]. Equation 2.14 is based upon an equation from literature and represents the oxygen demand as the ratio described [55].

$$OD = \frac{F_{out}(4x_{CH_4;out} + x_{CO;out} + x_{H_2;out})}{\frac{1000}{M_O}m_{fuel}} \quad (2.14)$$

In equation 2.14, F_{out} is the molar flow rate in the outlet, $x_{i;out}$ is the fraction of each species in the outlet gas, m_{fuel} is the amount of biomass in kg and M_O is the molar mass of oxygen. Finally, $\frac{1000}{M_O}$ is a constant which represents the amount of oxygen needed to burn the fuel. The value of this constant is based on findings in the literature for pine sawdust and is set to 1.5 [55]. OD is given in a value of the ratio of the oxygen demand per second, hence an integration of this equation with respect to time results in the total oxygen demand, τ for the system as represented in equation 2.15.

$$\tau = \int_0^{Z_t} OD dt \quad (2.15)$$

2.5 Analysis

Several different methods of analysis has been used to analyze fuel and the gases in the outlet as well as methods for further studies.

2.5.1 Thermogravimetric analysis

Thermogravimetric analysis, TGA, is a technique which studies the changes in physical and chemical properties of a sample. TGA measurements can be conducted through a temperature rise with a continuous heating rate, hence measurement as a function of temperature. It can also be performed as a function of time at which the temperature is held constant [56]. Furthermore, the TGA continuously measure the weight of the sample which creates a mass change profile as a function of either time or temperature. This curve is called the TG curve of which its derivative curve can also be produced [57]. The two curves provide the information necessary for the possibility of studying different physical and chemical phenomena. For physical phenomena these are for example vaporization and desorption while chemical phenomena include decomposition and dehydration. [56]

2.5.2 Infrared spectroscopy

Infrared (IR) spectroscopy emits IR radiation through a sample to analyze how much of the emitted radiation is absorbed into the sample at a particular wavelength. It is based upon the vibrations or rotations of atoms in a molecule which will vibrate at different energies. The energy absorbed corresponds to a certain frequency of vibration which can be analyzed. However, to be able to use this technique, the

electric dipole moment of the molecule must change when the IR radiation is absorbed. The frequencies recorded through using the IR spectroscopy can be used to identify different parts of or the entire molecule. By comparing the frequency to a register of what the different frequencies corresponds to, the composition of the sample can be determined. Some species which can be detected by IR are for example CO, CO₂, CH₄ and O₂ which are also the species analyzed in this thesis. [58]

2.5.3 Thermal conductivity

The thermal conductivity gas analysis is a method which is able to measure the concentration of gas by measuring the difference in thermal conductivity between the analyzed gas and a sample gas. The difference in thermal conductivity is measured through placing one platinum wire in contact with each gas and comparing the outcome. The process is able to measure the concentration continuously since the thermal conductivity simply changes when the concentration changes in the gas analyzed. The analysis method is able to detect species such as He, Ar and CH₄ but is in this thesis used for detecting H₂. [59]

2.5.4 Temperature programmed reduction

The method of temperature programmed reduction, TPR, is usually carried out to study how a metal oxide, typically a catalyst, is reduced at different temperatures [60]. The temperature in a TPR is increased linearly, usually 5-20°C per minute [61], which allows the study of how the temperature affects the reduction. Most commonly, hydrogen gas is used to reduce a catalyst to be able to gain knowledge into the behaviour of the catalyst. A thermal conductivity detector, described in section 2.5.3, is most commonly used in combination with a TPR to analyze the H₂ consumption during reduction. The results are presented as a plot between the consumption of H₂ and temperature. The peaks in these graphs are either different species or successive reduction of a particular species. However, in this thesis TPR will be used in a quite uncommon way which will be described in section 3.4.2. [60]

3

METHODOLOGY

In this chapter, firstly the reactor set up will be explained, followed by how the experiments were prepared with focus on the fuel and oxygen carrier. Finally, the conduction of the different experiments are described.

3.1 Experimental Setup

The reactor used in the experiments is made of quartz and is shown in figure 3.1. The reactor chamber is 200 mm high with a diameter of 36 mm while the gas inlet is 220 mm long. The distance between the two beds is 110 mm and from the top bed to the outlet 140 mm. The long gas inlet is used to allow for the gases to have time to be heated before reaching the first bed.

The entire experimental setup can be seen in figure 3.2 and begin with three gas cylinders with CO₂, air and N₂. The inlet gas is a mixture of N₂ and either air or CO₂. Depending on if the N₂ is mixed with air or CO₂ it either oxidizes the oxygen carrier or gases the fuel respectively. To choose if air or CO₂ is going through the system with N₂, a 3-way valve was used to easily change gases. The concentration and volumetric flows of N₂, air and CO₂ is decided through the valves and flow controllers seen in figure 3.2. Further, to combine and mix the gases after the 3-way valve, a T-connection and bomb is used. A bomb is an object shaped similar to a cylinder which mixes the gases.

When adding fuel to the reactor a purge flow is introduced to make sure that the fuel, as well as the volatiles created by the fuel, is pushed down towards the bottom bed. This purge flow has the same fractions as the oxidizing gas (inlet gas) has from below the reactor. The oxidizing gas and purge flow is split after the bomb, how high the flow rate is for each of these two flows is decided through one flow controller for each flow as shown in figure 3.2. The purge flow is introduced on top of the fuel chamber from where the fuel is fed into the reactor. How this system function during experiments will be described further in section 3.3.1.

The outlet gas leaves the reactor at the top. The gases are led into a condenser and particle filter after which it continues to two analyzers, one IR-analyzer (type ZRE) and one thermal conductivity detector (type ZAF) of which both are from Fuji Electric. The analyzers are able to present the data through logging one data point per second measuring the concentration of CH₄, H₂O, CO₂, H₂ and O₂. Finally,

3. Methodology

there is one additional opening at the top of the reactor, unmarked in the figure, which has been closed throughout all experiments.

Figure 3.1: The quartz reactor in the experimental setup.

Figure 3.2: The entire setup of the process.

3.2 Preparation of Experiments

Both the fuel and the oxygen carriers needed to be prepared before being able to be used in the experiments.

3.2.1 Fuel

The fuel used is sawdust from pine which was milled and sieved to three different ranges of particle size which were 500-1000, 1000-1700 and 1700-2000. These ranges are based on literature which recommend the particle size of pine sawdust fuel of between 500-2000µm [62] [55] [63] [64]. The biomass pine sawdust used was previously analyzed through a proximate and ultimate analysis by another member of the Chemical Engineering department at Monash University. The proximate analysis was conducted through using Thermogravimetric analysis (TGA) which was described in section 2.5.1. This analysis provides knowledge of what the fuel consist of in percentage of how much volatiles, char and ash which will be produced when running the experiments. The analysis reported that the volatile matter of the fuel is around 60 %, the char 23 % and ash 17 %, as can be seen in figure A.1

3. Methodology

in appendix A. Compared to literature, the amount of ash is slightly higher and amount of volatiles slightly lower.

The ultimate analysis provides an elemental composition of the fuel in terms of sulfur (S), carbon (C), hydrogen (H), nitrogen (N) and oxygen (O). The percentage of different constituents is presented in table 3.1 in which the percentage is on dry basis since the fuel in this thesis was dried prior to introducing it into the system. As the sum of the constituents is only 89.4 %_{dry}, there is 10.6 %_{dry} left. These are mostly constituents of the ash such as calcium, magnesium and iron.

Table 3.1: Dry basis percentage of constituents in solid fuel.

	% _{dry}
S	0.03
C	50
H	7
N	0.18
O	32.2
Sum	89.4

3.2.2 Oxygen carrier

Ilmenite and hematite were the oxygen carriers used which both had a particle size of between 150-250 μ m. The ilmenite used in this thesis is an Australian sand ilmenite mainly composed of FeO₃ (46.0 wt%) and TiO₂ (51.2 wt%). The hematite was obtained from Western Australia and is composed of mainly Fe₂O₃ (91.1 wt %). Ilmenite both has to be calcinated and activated before it is possible to use it for the best capacity possible, however this is not necessary for hematite. Instead hematite needs to be calcinated and deactivated. The hematite had already been calcinated by another member at Monash University before it was provided for these experiments. The deactivation was carried out to stabilize its reactivity through conducting a couple of reduction and oxidation cycles.

Ilmenite was calcinated through introducing it into the quartz reactor setup, previously described in section 3.1, and heating the system to 950. Air and N₂ was the oxidizing gases for which the mixture had a percentage of O₂ of around 5-7 %. The system was kept like this for about 4 hours. Activation of ilmenite was conducted through a series of reduction and oxidation cycles. The number of cycles was about 15 for which 40 g of oxygen carrier was activated at a time. The conditions were similar to those used during calcination for oxidation. During reduction, approximately 0.2 g of fuel was fed and around 50 vol % of CO was in the gas inlet.

3.3 Conduction of Experiments

A range of different experiments were carried out in the experimental setup previously explained. In this section, a description of an experimental cycle is given,

the values of parameters which are held constant are presented and the conducted experiments are described.

3.3.1 Description of an experimental cycle

Firstly, observe that these experiments are carried out in a batch procedure. The design of a cycle in this setup is to resemble a cycle of an oxygen carrier particle in a continuous interconnected reactor setup. One cycle of experiments include two parts; oxidation and reduction. Firstly, the oxidation is carried out in which N_2 and air is flown through the reactor at 950°C with enough flow rate to oxidize the oxygen carrier which is present on either both or one of the bottom or top bed. After about 10 minutes, all of the oxygen carrier should be oxidized and the system is ready to begin the reduction part. The 3-way valve is turned which leads to H_2 and CO_2 flowing through the system instead. Biomass is dried and the amount needed for the experiment is weighted. The biomass is placed above the closed screw-down valve which can be seen in figure 3.2 through removing the plug. As the purge gas is flown into the chamber, in which the biomass is kept, it pushes out the oxygen from the chamber by opening the plug slightly over the course of a minute. When no oxygen is present, the plug is kept closed and the screw-down valve is opened which causes the biomass to slide down into the reactor with the help of the purge gas. The volatiles generated by the biomass reacts with the oxygen in the oxygen carrier. When the vol% of CH_4 and CO is back at zero according to the analyzer and CO_2 is at its former inlet volumetric fraction, the reduction is completed. A second cycle can begin by turning the 3-way valve and introducing oxygen into the system to oxidize the oxygen carrier again as well as burning off any unconverted char.

3.3.2 Values of constant parameters

Throughout the experiments the temperature, concentration of CO_2 total flow rate, concentration of O_2 , particle size and purge flow rate were kept around the same value which is presented in table 3.2. The temperature recommended by literature is by several articles exemplified to 950°C to run a CLC process on [63] [65] [43], which is why this temperature was chosen for all experiments. The temperature could not be continuously measured throughout the cycles. Instead, the temperature was measured as the reactor was heated up. When the reactor was heated up, the system was closed and after a number of cycles the system was opened again to control the temperature. The temperature inside the reactor was operated by manually change the temperature target of the oven. As the system was well insulated the temperature in the reactor was contained within a span of 1°C from 950. The concentration of CO_2 in the gas inlet mixed with nitrogen gas has not been thoroughly studied by literature before. The concentration ranges from 39 vol%, in an article which introduces oxygen as well, to 75 vol% with a CLOU conversion process [66] [67]. The concentration in this thesis was decided to be between 45 vol% and 50%.

3. Methodology

Further, all experiments have had approximately the same total flow rate of 2.7 L/min, give or take 0.3 L/min, which was based upon the minimum fluidization velocity and what flow rates the experimental setup could work in. 2.7 L/min corresponds to a velocity of $1.99U_{mf}$ which means that the flow rate is about 2 times higher than the minimum fluidization velocity U_{mf} which was calculated to 0.022 m/s. During re-oxidation of the oxygen carrier, the same percentage of O_2 as during activation was used which was 5-7 %. The percentage of oxygen is kept relatively low as heat is produced during reaction with the oxygen carrier. As the heat is produced, the temperature rises and if it becomes too high it may damage the oxygen carrier. Further, the particle size of the pine sawdust was kept at 1700-2000 μm after qualitative testing. Similar qualitative testing was conducted for deciding upon a purge flow which was after those experiments decided to 0.9 L/min. Observe that the purge flow is a part of the total flow of 2.7 L/min, hence the flow when the purge flow is closed to put biomass into the chamber from where it is fed, the total flow rate decreases to 1.8 L/min which corresponds to a velocity which is still above the minimum fluidization velocity. Hence, there are three parts of one experimental cycle which uses the constant parameters, mentioned in this section, differently. During re-oxidation for example there is no CO present and as just mentioned, an open or closed purge lead to a different total flow rate. The three parts of the cycle are concluded in table 3.2 and consist of the re-oxidation of the oxygen carrier, the reduction phase without purge flow into the system (when loading the fuel) and finally the reduction phase with the purge flow (when feeding the fuel).

Table 3.2: Values of the parameters kept constant throughout all experiments during different parts of the experimental cycle.

	Re-oxidation	Loading fuel	Feeding fuel
Temperature [°C]	950	950	950
Concentration of CO_2 [vol%]	0	45-50	45-50
Total flow rate [L/min]	2.7	1.8	2.7
Concentration of O_2 [vol%]	5-7	0	0
Particle size [μm]	1700-2000	1700-2000	1700-2000
Purge flow rate [L/min]	0.9	0	0.9

3.3.3 Gas composition

To know how much of the constituents from the devolatilization process that have reacted, an experiment without any oxygen carrier was conducted. The experiment was carried out at the same conditions as described in section 3.3.2. The amount of biomass that was introduced into the system for this experiment was 0.15 g. The particle size was 1700-2000 μm and the purge flow was 0.9 L/min.

3.3.4 Optimization of experimental parameters

There were four different parameters which were tested in the optimization of the experimental parameters, these were particle size, dual or single bed, residence time and the fuel/OC ratio. To the extent possible, all parameters except the one studied

were kept constant. Hence, only the parameter studied in the particular experiment was varied.

3.3.4.1 Particle size and purge flow rate

Firstly, the particle size of the fuel was optimized by testing three different ranges of size mentioned in 3.2.1. These were 500-1000, 1000-1700 and 1700-2000. Feeding the fuel of different particle sizes were conducted on a qualitative basis where several cycles with different amount of purge gas was used to observe which particle size was best for this particular setup. The purge flow needed to be high enough to help push the biomass into the reactor, but wanted to be kept low to keep a high residence time between the gas and the oxygen carrier. The amount of purge flow ranged from 0-1.25 L/min. The results from these experiments will be used for all other experiments in the following sections which is why they were presented in section 3.3.2.

3.3.4.2 Dual or single fluidizing bed

As shown in figure 3.1, the bottom bed is located just below where the fuel is fed while the top bed is located above the fuel inlet. Three different configurations have been carried out to analyze whether or not there is a difference in results when more oxygen carrier is present in the top bed. The same fuel/OC ratio, at 0.00375, was kept throughout the experiments corresponding to 0.15 g of biomass which was fed every cycle with a total of 40 g of ilmenite being present in the system. The three different configurations which were tested are presented in table 3.3 showing the amount of ilmenite added to each bed.

Table 3.3: The different configurations for analyzing dual or single bed options.

Configuration	Top bed	Bottom bed
All top	40 g	0 g
75/25	30 g	10 g
50/50	20 g	20 g

3.3.4.3 Residence time

The residence time that the gas from the fuel is in contact with the oxygen carrier is dependent upon the flow rate and the height of the bed. Due to results from the previous experiments in this thesis, only the top bed was used since it performs the best. Approximately the same flow rate at around 2.7 L/min was kept throughout the experiments and hence the only way that the residence time was increased was through increasing the amount of ilmenite in the top bed. The more the oxygen carrier, the higher the bed height and hence the longer residence time. The maximum bed height possible in the setup corresponds to using 60 g of oxygen carrier. A higher amount would lead to too high loss of oxygen carrier as when the oxygen carrier fluidizes it has the risk of leaving the system with the gases. The experimental configurations is presented in table 3.4 which uses 20, 40 and 60 grams of ilmenite to vary residence time but keeps the fuel/OC ratio the same at 0.00375.

3. Methodology

Table 3.4: The different configurations for analyzing residence time.

Amount of oxygen carrier	Amount of biomass
20 g	0.075 g
40 g	0.15 g
60 g	0.225 g

3.3.4.4 Fuel/OC ratio

The ratio between the amount of fuel and the amount of oxygen carrier was studied. In literature the ratio 0.005 has been found between fuel and oxygen carrier. In which their process had other types of fuel than biomass though but used ilmenite as oxygen carrier [65]. Due to limitations in how much fuel that can be fed to the system, the upper limit has had to be 0.01. Therefore, the chosen range to test the ratio was decided to be 0.00375 to 0.01. In table 3.5, the four different fuel/OC ratios tested can be seen with corresponding amount of fuel where all of the experiments were carried out with 20 g of ilmenite placed in the top bed.

Table 3.5: The different fuel/OC ratios with corresponding amount of fuel.

Fuel/OC ratio	Fuel
0.00375	0.075 g
0.005	0.1 g
0.00625	0.125 g
0.01	0.2 g

3.3.5 Residence time using hematite

To be able to compare the results with a second oxygen carrier, hematite was used as well. The experiments focuses on how the residence time influences the results for hematite and need to be able to be compared to the results from ilmenite. Hence, exactly the same procedure as was presented in in section 3.3.4.3 was used.

3.4 Other Setups and Methods used

During the master thesis work, two other experimental setups has been used, one metallic reactor and the analysis method temperature programmed reduction.

3.4.1 Metallic reactor

A larger reactor made of high-temperature stainless steel was used in the beginning to perform experiments which is shown in figure 3.3. The reactor had an inner diameter of 50 mm and was 970 mm tall. There were several problems which arose when trying to use this reactor. The bed was attached to a metallic cylinder, shown in figure 3.4 with high temperature cement. However, the cement was, after drying, quite brittle which led to it easily breaking when introducing it into the rest of the

reactor. The cylinder was exactly the right dimensions to slide it with some force into the reactor, using a form of lube. As force had to be used there was a high risk for the cement to break and hence the bed could become loose, creating pathways for the gas to pass beside the bed instead of through it. Further, two different beds were tested. First, a sintered plate with 40 μ m pores made out of brass. It was said that as it was sintered it could withstand higher temperatures than brass otherwise could. This turned out to be false as the brass sintered plate fell apart after a number of tries to calcinate the oxygen carrier. A new sintered plate was tested, made from stainless steel with 20 μ m pores. The new sintered plate worked better, as it could withstand the heat, however the solution of attaching the bed with cement was not reliable and after many failed attempts the metallic reactor was finally changed into using the smaller quartz reactor described in section 3.1 instead.

Figure 3.4: The smaller cylinder which slides into the larger part of the reactor with a bed attached to it through cement.

Figure 3.3: The metallic reactor which was used in initial experiments.

3.4.2 Temperature programmed reduction

The TPR was used in a quite unconventional way to take the studies of the effect of increased residence time one step further. The TPR is made up from a U-shaped quartz tube with a bed which is inside an oven. Although the TPR is commonly used with successive heating and analysis, in these experiments it was kept isothermal at 950 °C. Before the quartz tube, a helium and air cylinder is present. In between these, there is a possibility to inject gas through a syringe to introduce other types of gas into the system. Finally, after the quartz tube, the gas continues into an

3. Methodology

analyzer. The setup is shown in figure 3.5

Figure 3.5: The setup in the TPR experiments.

1 gram active ilmenite was placed on the bed inside the quartz tube. While flowing pure helium a small volume (0.4 ml - 2 ml) of pure CO was injected using a syringe. Hence using the low flow rate in the TPR, the residence time between the CO and the oxygen carrier can be significantly higher than in the quartz reactor. To evaluate the increased residence time, the plan was to change the total flow rate and find a correlation between the residence time and the conversion of the injected CO. After the CO was injected, the flowing gas was changed from helium to air in order to re-oxidize the oxygen carrier. After that, the oxygen carrier was fully oxidized the cycle was repeated. Some trials to re-oxidize the ilmenite by injecting the air instead of changing the inlet gas from He was conducted. This method was tried in order to calculate how much air it was needed to re-oxidize the ilmenite and use it to determine the amount of oxygen consumed in one cycle. The consumed oxygen corresponds directly to the conversion of CO. However, some problems arose while using these methods and no conclusive results could be gained, the problems are described in section 4.4.2.

4

RESULTS AND DISCUSSION

This chapter includes the results and discussion regarding gas composition, the optimization of process parameters and finally the residence and comparison using hematite.

4.1 Gas Composition

Figure 4.1 shows a graph over time for the procedure described in section 3.3.3. A high peak of CO can be observed and is noted that a significant part of the volatiles in the biomass is from CO. Smaller peaks of C_4H_2 and CO_2 are also present which is consistent with literature specifying the volatiles of biomass to be CO, C_4H_2 and CO_2 . The experiment which was carried out for the results showed in figure 4.1 was conducted at the beginning of the experimental procedures. Relatively quickly afterwards experiments with oxygen carrier present were carried out in which H_2 was detected by the analyzer. These results led to the conclusion that the reaction between H_2 and the oxygen carrier was quick enough for all of the H_2 to react, especially since H_2 had been observed in the gas composition experiments. However, new gas composition experiments, without oxygen or oxygen carrier in the system, were run in the end of the master thesis for some additional results when it was noted that no H_2 was observed by the analyzer. After several more experiments and further attempts at problem solving no reason could be found other than that there might be a problem with the gas analyzer. Hence, there is little knowledge of when this problem arose during the experiments carried out for this master thesis. Due to the fact that no H_2 was observed in experiments that were conducted shortly after the first gas composition experiment, it is with confidence that it is believed that all H_2 in all the following experiments (except the gas composition experiment) did indeed react and is the reason why it is not present in any of the analysis. Hence, there is very little reason to not trust the results expressed in conversion of CO. However, the results of the total oxygen demand is a function of the fraction of H_2 in the outlet which is zero in all of our results. Hence, these specific results should be able to be trusted as well, especially the trends that the results show of the total oxygen demand.

Figure 4.1: A graph of the gas composition over time for biomass.

Further, from the later experiments concerning the gas composition the amount of CO, which is generated by the biomass fuel, was calculated. The amount of CO per gram of biomass is 0.5203 g, hence about 52 wt%.

4.2 Optimization of Experimental Parameters

The results of the four different optimization procedures that were presented in section 3.3.4 are presented in this section along with some discussion. The results presented are focused on the conversion of CO and the total oxygen demand. To show examples of the data which the calculations are based upon, two graphs, figure 4.2 and 4.3, are given as an example. Figure 4.2 show how the composition in vol% changes over time during a reduction cycle which is the basis for both the calculation of conversion of CO and the total oxygen demand. Notice that the vol% of CO decreases, this is due to that it is consumed during gasification of the char but mainly because other gases are produced which decreases its vol%. Figure 4.3 show how the oxygen demand changes over time and is integrated to calculate the total oxygen demand. As can be expected, the oxygen demand is at it's largest by the same time as the uncombusted volatiles are detected by the analyzer. The two graphs shown are based upon two different cycles.

Figure 4.2: The composition of the different gases in the outlet during a reduction cycle.

Figure 4.3: The oxygen demand over time for a reduction cycle.

4.2.1 Particle size and purge flow rate

As described in section 3.3.4.1 the choice of particle size and purge flow rate was based upon a qualitative assessment on how well the biomass could be fed in the reactor setup. The drawback with the larger particle sizes are that they potentially

4. Results and Discussion

get stuck in the laboratory equipment which guides the fuel down into the reactor. The drawback on the other hand with the smaller particle sizes is that it weighs less and hence does not fall down towards the reactor as easily. Problems were identified with all particle sizes but 1700-2000 μm was decided upon being the best to feed through the system. It was chosen because it was the most reliable to be able to gain a rather constant flow of biomass fed into the system in a similar way so it does not differ too much in between the different cycles.

Further, the purge flow need to be high enough to push down the biomass and the volatiles released. If it is too high however, a too low flow rate might be present when the purge flow is cut off. Hence, there must be a balance of how high the flow rate can be in the flow rate. After testing different flow rates it could be noted that about 0.9 L/min would be preferable as this is high enough to push the biomass downwards but leaves the total flow rate high enough to be able to fluidize the oxygen carrier when the purge is shut off. In another set up, it would be interesting to study if the particle size and flow of purge gas would influence the results in terms of conversion of CO and oxygen demand rather than qualitatively. In this set up, it was not possible as the cycles carried out with smaller particle size and less purge gas flow were hard to carry out and the biomass did not enter the reactor smoothly.

4.2.2 Dual or single fluidizing bed

The conversion of CO and total oxygen demand for each of the three configurations are presented in figures 4.4 and 4.5 in which each circle represents the results from one cycle. A clear trend can be seen in which higher conversion can be seen the more of the oxygen carrier that is present in the top bed. Since biomass has a high degree of volatiles, the results can be explained by that the volatiles are released so fast from the biomass that they do not come in contact with the oxygen carriers in the bottom bed to the same degree as it does in the top bed. Although the conversion is relatively low for all configurations, keeping all the oxygen carrier in the top bed leads to almost twice as high conversion as compared to the configuration with 50 % in the top bed. Further, the total oxygen demand decreases the more of the oxygen carrier which is present in the top bed which also implies that more oxygen needs to be present in the system. As more oxygen, through the oxygen carrier, is present in the top bed, the total oxygen demand decreases. Hence the measurements of conversion of CO and the total oxygen demand show clear benefits with placing all oxygen carrier in the top bed of the reactor.

Figure 4.4: The conversion of CO with increasing amount of oxygen carrier in top bed.

Figure 4.5: The total oxygen demand with increasing amount of oxygen carrier in top bed.

4.2.3 Residence time

By increasing the time of which the volatiles from the fuel can be in contact with the oxygen carrier, a higher conversion of CO is possible which can be seen in figure 4.6.

4. Results and Discussion

Further, as more of the volatiles are converted, less oxygen is demanded and hence the total oxygen demand for the cycle decreases with increasing residence time as seen in figure 4.7. As explained in section 3.3.4.3, the residence time is increased through increasing the bed height by changing the amount of oxygen carrier. Hence, these results also support the findings in section 4.2.2 since a similar situation arise in those experiments. A higher percentage of the oxygen carrier which is present in the top bed leads to a longer residence time for the volatiles to pass through the oxygen carrier as little seems to pass the bottom bed. Although, the total oxygen demand does not differ as much percentage-wise it still shows a clear trend that it is decreasing with increasing residence time. Therefore, it is clear that a higher residence time creates beneficial conditions for the volatiles generated by the biomass to react.

Figure 4.6: The conversion of CO with increasing residence time.

Figure 4.7: The total oxygen demand with increasing residence time.

4.2.4 Fuel/OC ratio

The results from increasing the fuel/OC ratio are shown in figures 4.8 and 4.9. The amount of fuel in each configuration increases with increasing fuel/OC ratio. With a higher fuel/OC ratio, the conversion of CO increases while the total oxygen demand decreases. The conversion of CO increases significantly, especially if comparing the ratio 0.00375 with 0.01, with an amount similar to the change in conversion of CO when increasing the residence time from using 20 to 60 g of oxygen carrier. Meanwhile, the total oxygen demand shows a clear trend of decreasing with higher fuel/OC ratio although the difference in percentage is relatively low similar to the case of increasing residence time. Since the maximum fuel/OC ratio that was possible to use was 0.01 it is not known what happens at higher ratios. As can be seen by these results the conversion of CO and oxygen demand might increase and decrease respectively when increasing the ratio a bit more. However, at a certain point these results should instead start to decrease and increase respectively as there will be a limit to the amount of fuel that the oxygen carrier can take care of. Using a high as possible fuel/OC ratio would be of great importance in a larger scale system as it would both increase the conversion of CO but also the amount of fuel which could be combusted per cycle.

Figure 4.8: The conversion of CO with increasing fuel/OC ratio.

Figure 4.9: The total oxygen demand with increasing fuel/OC ratio.

As can be noted, there are results missing at the fuel/OC ratios of 0.0075 and 0.00875. The plan was to carry out these experiments as well, however there was both a lack of time and problems with the experimental setup which hindered conduction of these experiments. Although there are missing values, there is still a clear trend which can be observed in these two graphs. It is suspected that the two missing fuel/OC ratios would lie along the same trend if it would have been possible

to perform them.

4.3 Residence Time using Hematite

The results of the experiments when working with hematite and an increasing residence time show a similar trend to the results of ilmenite. An increasing amount of oxygen carrier, hence increasing the residence time, increases the conversion of CO and decreases the total oxygen demand as can be seen in figures 4.10 and 4.11.

Figure 4.10: The conversion of CO for hematite with increasing residence time.

Figure 4.11: The total oxygen demand for hematite with increasing residence time.

Compared to ilmenite, hematite shows significantly better results for both the conversion of CO and the oxygen demand which is shown in figures 4.12 and 4.13. While the conversion of CO for ilmenite increases from about 15 to 38 % with increasing residence time, the conversion of CO for hematite increased from around 22 up to around 60 % instead. Further, the total oxygen demand for both ilmenite and hematite start at around 55 to 60 %, but the total oxygen demand for hematite decreases more significantly with higher amounts of oxygen carrier and reaches around 35 % while the same amount of ilmenite only reaches 50 %. Notably, the difference in percentages from the lowest to highest for both conversion of CO and the total oxygen demand is significantly bigger for hematite. Hence, hematite seem to act as a significantly better oxygen carrier when it comes to these two measurements of results.

Figure 4.12: The conversion of CO for both ilmenite and hematite with increasing residence time.

Figure 4.13: The total oxygen demand for both ilmenite and hematite with increasing residence time.

4.4 Other Setups and Methods used

The results from the other setups used through this thesis will be presented including the metallic reactor and TPR setup described in section 3.4.

4.4.1 Metallic reactor

Unfortunately no results were able to be gained from using the setup with the larger metallic reactor. As described in section 3.4.1, the cement holding the bed in place broke multiple times. Also, the bed which was used in the beginning had a too low melting point, these were the two main reasons for why no results could be obtained using this setup. It was at one point possible to calcinate the oxygen carrier in this setup but particles from cement which broke mixed in with the calcinated oxygen carrier. This led to that the oxygen carrier was discarded. No activation or other experiments were carried out in this reactor, which also means that no data logging by analyzers were carried out. Hence, there are no quantitative results which can be shown.

4.4.2 Temperature programmed reduction

To analyze the increased residence time between the ilmenite and CO a small volume of CO was injected to the TPR. A problem which arose was that the thermal conductivity analyzer used could not detect the difference between CO and CO_2 in the outlet gas. In the generated data from the experiments there was just one peak which corresponds to both CO and CO_2 . Meaning that the conversion of CO could not be calculated. The results from these experiments could therefore not be used.

Further, the plan of changing the analyzer could unfortunately not be carried out because of software problems. Another way to solve this problem was through trials of oxidizing the oxygen carrier by injecting pulses of air. Since it would then be known how much of the oxygen which is oxidizing the oxygen carrier. With those results, the corresponding amount of CO or CO_2 could be calculated. The result from this method however was not considered to be reliable enough for further studies due to big variations in the generated data.

5

CONCLUSION

The aim of this thesis had multiple objectives focusing on the usage of biomass in a CLC system and how the large amount of volatiles could be handled. Furthermore, it also included studies on how the experimental setup should be used for the most optimal results.

Firstly, the particle size together with the purge gas flow rate was qualitatively studied. In these particular experiments a particle size of 1700-2000 μ m was found the most optimal in combination with a purge gas flow of about 0.9 L/min. Notice however that this is particular for the system used in this thesis and may not be applicable for other experimental setups.

Secondly, using both the bottom and top bed or only the top bed was studied. It was shown that using only the top bed led to significantly higher conversion of CO and a lower oxygen demand due to the high amount of volatiles quickly released from the biomass. As more oxygen carrier is present in the top bed, it increases the residence time of the volatiles in contact with the oxygen carrier, which was further studied.

Thirdly, it was shown with confidence that the higher the residence time, the higher the conversion of CO and the lower the oxygen demand. Hence, it is important to keep the residence time in a CLC system as long as possible to create beneficial conditions for the volatiles to react, especially when using biomass or another fuel with a high fraction of volatiles.

Fourthly, when the ratio between the amount of fuel and the amount of oxygen carrier increases the results improve as well. That is, the conversion of CO increases and the oxygen demand decreases. This trend cannot continue for long and hence further studies to optimize this parameter should be carried out which will be described in section 5.1. A high as possible fuel/OC ratio would be beneficial in a process due to the higher efficiency which it creates.

Finally, hematite was used to study both its trends with regards to residence time as well as being able to compare it to ilmenite. Hematite showed the same trend compared to ilmenite but had significantly better values. A much higher conversion of CO as well as a lower oxygen demand.

5.1 Future Work

There is a lot of research which can be carried out within this field in the future. Some of the potential research subjects which were identified through analysis of the results will be presented in this section.

As the particle size was only studied through qualitative measures it would be of interest to study if the difference in particle size would influence the results quantitatively as well. A smaller particle size could lead to faster generation of volatiles from the fuel for example which could influence the results.

Since the results improve with an increased residence time it would be of interest to conduct a more specific study within this area. There are multiple other ways to increase residence time apart from increasing the amount of fuel which was used in this thesis. For example, decreasing the flow rate through the system and using different reactor designs influences the residence time. Further, even longer residence times should be studied to analyze when the residence time becomes unnecessarily long. To create an efficient system, there must be a balance between how long residence time is used against for example cost of the system. This is especially important for commercial processes which it should be studied for as well. This type of study could most likely be performed through the use of a TPR as described in section 3.4.2. Hence, it is recommended to conduct further research into using this method.

Finally, as the results in this thesis have improved with increasing fuel/OC ratio, it is of interest to conduct further research within this area. In the setup used in this thesis there was a limit of how high fuel/OC ratios that were possible, therefore it would be of interest to increase the ratio further. At some point there should be an optimal ratio which would be beneficial to find to be able to use the CLC system as efficiently as possible.

BIBLIOGRAPHY

- [1] IPCC. Climate Change 2014 Synthesis Report. Contribution of Working Groups I, II and III to the Fifth Assessment Report of the Intergovernmental Panel on Climate Change [Core Writing Team, R.K. Pachauri and L.A. Meyer (eds.)]. IPCC, Geneva, Switzerland, 151 pp.; 2014.
- [2] The United Nations, Paris agreement , 2015;.
- [3] ESRL. ESRL Global Monitoring Division News Items; 2013. Available from: <https://www.esrl.noaa.gov/gmd/news/7074.html> .
- [4] ESRL. ESRL Global Monitoring Division - Global Greenhouse Gas Reference Network; 2019. Available from: <https://www.esrl.noaa.gov/gmd/ccgg/trends/global.html> .
- [5] Clapp C, Francke Lund H, Aamaas B, Lannoo E. Shades of Climate Risk: Categorizing climate risk for investors. 2017 02;.
- [6] IEA. Carbon capture, utilisation and storage: A critical tool in the climate energy toolbox; 2018. Available from: <https://www.iea.org/topics/carbon-capture-and-storage/> .
- [7] CCSA. What is CCS?; 2019. Available from: <http://www.ccsassociation.org/what-is-ccs/?fbclid=IwAR1fXiwNgZfzIVI3UUJddUEPjyhTXzoVf2PJHtWAQVJ0ZdJPyVQOE5Gsn8>
- [8] Palm E, Nilsson L, Åhman M. Electricity-based plastics and their potential demand for electricity and carbon dioxide. Journal of Cleaner Production. 2016;129:548-555.
- [9] Timmins G. CCU: a viable weapon in the fight against climate change?; 2019. Available from: https://www.imperial.ac.uk/news/178646/ccu-viable-weapon-fight-against-climate/?fbclid=IwAR3x-Y8TV0hRXA9sBoWY0pLok_SqNcwE9dIVEN0mH5TEOLV8mt6wM-SyoLo
- [10] Bui M, Fajardy M, Dowell NM. Bio-energy with carbon capture and storage (BECCS): Opportunities for performance improvement. Fuel. 2018;213:164-175.
- [11] Herzog H, Golomb D. Carbon Capture and Storage from Fossil Fuel Use. Encyclopedia of Energy. 2004;1:277-287.
- [12] Gibbins J, Chalmers H. Carbon capture and storage. Energy Policy. 2008;36(12):4317-4322.
- [13] Jiang S, Shen L, Wu J, Yan J, Song T. The investigations of hematite-CuO oxygen carrier in chemical looping combustion. Chemical Engineering Journal. 2017;317:132-142.
- [14] Abad A, García-Labiano F, Gayán P, de Diego LF, Adánez J. Redox kinetics of $\text{CaMg}_{0.1}\text{Ti}_{0.125}\text{Mn}_{0.775}\text{O}_{2.9}$ for Chemical Looping Combustion (CLC) and

- Chemical Looping with Oxygen Uncoupling (CLOU). *Chemical Engineering Journal*. 2015;269:67–81.
- [15] Lyngfelt A. Chemical-looping combustion of solid fuels – Status of development. *Applied Energy*. 2014;113:1869–1873.
- [16] Ulloa CA, Gordon AL, García XA. Thermogravimetric study of interactions in the pyrolysis of blends of coal with radiata pine sawdust. *Fuel Processing Technology*. 2009;90:583–590.
- [17] Adánez-Rubio I, Abad A, Gayán P, de Diego LF, García-Labiano F, Adánez J. Performance of CLOU process in the combustion of different types of coal with CO₂ capture. *International Journal of Greenhouse Gas Control*. 2013;12:430–440.
- [18] García R, Pizarro C, Lavín AG, Bueno JL. Biomass proximate analysis using thermogravimetry. *Bioresource Technology*. 2013;139:1–4.
- [19] Ping W, Nicholas M, Dushyant S, David B, Mehrdad M. Chemical-Looping Combustion and Gasification of Coals and Oxygen Carrier Development: A Brief Review. *Energies*, Vol 8, Iss 10, Pp 10605-10635 (2015). 2015;(10):10605.
- [20] Moldenhauer P, Sundqvist S, Mattisson T, Linderholm C. Chemical-looping combustion of synthetic biomass-volatiles with manganese-ore oxygen carriers. *International Journal of Greenhouse Gas Control*. 2018;71:239–252.
- [21] Lyngfelt A, Linderholm C. Chemical-Looping Combustion of Solid Fuels Status and Recent Progress. *Energy Procedia*. 2017;114:371–386. 13th International Conference on Greenhouse Gas Control Technologies, GHGT-13, 14-18 November 2016, Lausanne, Switzerland.
- [22] Zhao X, Zhou H, Sikarwar V, Zhao M, Park AH, Fennell P, et al. Biomass-based chemical looping technologies: The good, the bad and the future. *Energy & Environmental Science*. 2017 05;10.
- [23] Adanez J, Abad A, Garcia-Labiano F, Gayan P, De Diego LF. Progress in Chemical-Looping Combustion and Reforming technologies. *Progress in Energy and Combustion Science*. 2012;(2):215.
- [24] Wang P, Means N, Howard BH, Shekhawat D, Berry D. The reactivity of CuO oxygen carrier and coal in Chemical-Looping with Oxygen Uncoupled (CLOU) and In-situ Gasification Chemical-Looping Combustion (iG-CLC). *Fuel*. 2018;217:642–649.
- [25] Kunii D, Levenspiel O. CHAPTER 1 - Introduction. In: Kunii D, Levenspiel O, editors. *Fluidization Engineering (Second Edition)*. second edition ed. Boston: Butterworth-Heinemann; 1991. p. 1–13.
- [26] Kimball E, Hamers HP, Cobden P, Gallucci F, van Sint Annaland M. Operation of fixed-bed chemical looping combustion. *Energy Procedia*. 2013;37:575–579. Available from <http://www.sciencedirect.com/science/article/pii/S1876610213001549>.
- [27] Meng WX, Banerjee S, Zhang X, Agarwal RK. Process simulation of multi-stage chemical-looping combustion using Aspen Plus. *Energy*. 2015;90:1869–1877.
- [28] Coppola A, Solimene R, Bareschino P, Salatino P. Mathematical modeling of a two-stage fuel reactor for chemical looping combustion with oxygen uncoupling of solid fuels. 2015 04;157.

- [29] Zhao Z, Iloeje CO, Chen T, Ghoniem AF. Design of a rotary reactor for chemical-looping combustion. Part 1: Fundamentals and design methodology. *Fuel*. 2014;121:327–343.
- [30] Tijani MM, Aqsha A, Mahinpey N. Synthesis and study of metal-based oxygen carriers (Cu, Co, Fe, Ni) and their interaction with supported metal oxides (Al₂O₃, CeO₂, TiO₂, ZrO₂) in a chemical looping combustion system. *Energy*. 2017;138:873–882.
- [31] Li J, Zhang H, Gao Z, Fu J, Ao W, Dai J. CO₂ Capture with Chemical Looping Combustion of Gaseous Fuels: An Overview. *Energy & Fuels*. 2017;31(4):3475–3524.
- [32] Forutan HR, Karimi E, Ha zi A, Rahimpour MR, Keshavarz P. Expert representation chemical looping reforming: A comparative study of Fe, Mn, Co and Cu as oxygen carriers supported on Al₂O₃. *Journal of Industrial and Engineering Chemistry*. 2015;21:900–911.
- [33] Feng Y, Guo X. Study of reaction mechanism of methane conversion over Ni-based oxygen carrier in chemical looping reforming. *Fuel*. 2017;210:866–872.
- [34] Dueso C, Izquierdo MT, García-Labiano F, de Diego LF, Abad A, Gayán P, et al. Effect of H₂S on the behaviour of an impregnated NiO-based oxygen-carrier for chemical-looping combustion (CLC). *Applied Catalysis B: Environmental*. 2012;126:186–199.
- [35] Adánez-Rubio I, Izquierdo MT, Abad A, Gayán P, de Diego LF, Adánez J. Spray granulated Cu-Mn oxygen carrier for chemical looping with oxygen uncoupling (CLOU) process. *International Journal of Greenhouse Gas Control*. 2017;65:76–85.
- [36] Sundqvist S, Arjmand M, Mattisson T, Rydén M, Lyngfelt A. Screening of different manganese ores for chemical-looping combustion (CLC) and chemical-looping with oxygen uncoupling (CLOU). *International Journal of Greenhouse Gas Control*. 2015;43:179–188.
- [37] Adánez J, Abad A, Mendiara T, Gayán P, de Diego LF, García-Labiano F. Chemical looping combustion of solid fuels. *Progress in Energy and Combustion Science*. 2018;65:6–66.
- [38] Chemlink; 2019. Available from: http://www.chemlink.com.au/titan_rutile.htm.
- [39] Bhogeswara Rao D, Rigaud M. Kinetics of the oxidation of ilmenite. *Oxidation of Metals*. 1975;9(1):99.
- [40] Schwebel GL, Leion H, Krumm W. Comparison of natural ilmenites as oxygen carriers in chemical-looping combustion and influence of water gas shift reaction on gas composition. *Chemical Engineering Research and Design*. 2012;90(9):1351–1360.
- [41] Corcoran A, Knutsson P, Lind F, Thunman H. Comparing the structural development of sand and rock ilmenite during long-term exposure in a biomass fired 12MWth CFB-boiler. *Fuel Processing Technology*. 2018;171:39–44.
- [42] Cuadrat Fernández A, Adánez Elorza J, Abad Secades A. Chemical-looping combustion of coal using ilmenite as oxygen-carrier. *Universidad de Zaragoza*;

- [43] Adanez J, Cuadrat A, Abad A, Gayan P, de Diego LF, Garcia-Labiano F. Ilmenite Activation during Consecutive Redox Cycles in Chemical-Looping Combustion. *Energy and Fuels*. 2010;(1):1402.
- [44] Niu X, Shen L, Gu H, Jiang S, Xiao J. Characteristics of hematite and fly ash during chemical looping combustion of sewage sludge. *Chemical Engineering Journal*. 2015;268:236 – 244.
- [45] GeoscienceAustralia. Iron Ore - AIMR 2011 - Australian Mines Atlas; 2019. Available from: http://www.australianminesatlas.gov.au/aimr/commodity/iron_ore.html.
- [46] Huang Z, He F, Feng Y, Zhao K, Zheng A, Chang S, et al. Synthesis gas production through biomass direct chemical looping conversion with natural hematite as an oxygen carrier. *Bioresource Technology*. 2013;140:138 – 145.
- [47] Monazam ER, Breault RW, Siriwardane R. Kinetics of Magnetite (Fe₃O₄) Oxidation to Hematite (Fe₂O₃) in Air for Chemical Looping Combustion. *Industrial & Engineering Chemistry Research*. 2014;53(34):13320–13328.
- [48] Barthelmy D. Magnetite Mineral Data; 2019. Available from: <http://www.webmineral.com/data/Magnetite.shtml#.XPCJDhMza3U>.
- [49] Hamers HP, Romano MC, Spallina V, Chiesa P, Gallucci F, van Sint Annaland M. Energy analysis of two stage packed-bed chemical looping combustion configurations for integrated gasification combined cycles. *Energy*. 2015;85:489 – 502.
- [50] Langørgen Ø, Saanum I, Haugen NEL. Chemical Looping Combustion of Methane Using a Copper-based Oxygen Carrier in a 150 kW Reactor System. *Energy Procedia*. 2017;114(13th International Conference on Greenhouse Gas Control Technologies, GHGT-13, 14-18 November 2016, Lausanne, Switzerland):352 – 360.
- [51] ABARES. Australia's State of the Forests Report 2018 - Australian Bureau of Agricultural and Resource Economics and Sciences; 2018.
- [52] Strömberg B, Svärd SH. Infrared spectroscopy. [electronic resource] : fundamentals and applications. *Analytical techniques in the sciences*. Chichester, West Sussex, England ; Hoboken, NJ : J. Wiley, c2004.; 2004.
- [53] Anantharaman A, Cocco RA, Chew JW. Evaluation of correlations for minimum fluidization velocity (U_{mf}) in gas-solid fluidization. *Powder Technology*. 2018;323:454 – 485.
- [54] Wen CY, Yu YH. A generalized method for predicting the minimum fluidization velocity. *AIChE Journal*. 1966 5;12(3):610–612.
- [55] Mendiara T, Pérez-Astray A, Izquierdo MT, Abad A, de Diego LF, García-Labiano F, et al. Chemical Looping Combustion of different types of biomass in a 0.5 kW_{th} unit. *Fuel*. 2018;211:868–875.
- [56] Vyazovkin S, Koga N, Schick C. In: 13.3.6 Thermogravimetric Analysis (TGA). Elsevier; 2019. .
- [57] Pandey A, Bhaskar T, Stöcker M, Sukumaran Rajeev K. In: 3.3.2 Thermogravimetric Analysis of Biomass. Elsevier; 2015. .
- [58] Stuart B. Infrared spectroscopy. [electronic resource] : fundamentals and applications. *Analytical techniques in the sciences*. Chichester, West Sussex, England ; Hoboken, NJ : J. Wiley, c2004.; 2004.

-
- [59] Thermal Conductivity Gas Analyzer ZAF - Fuji Electric; 2019. Available from: https://www.fujielectric.com/products/instruments/products/anz_gas/ZAF.html.
- [60] Murzin Dmitry Y. In: 2.2.5.1 Temperature-Programmed Reduction. De Gruyter; 2014. .
- [61] Kamer Paul C J, Vogt D, Thybaut Joris W. In: 23.2 Temperature Programmed Reduction (TPR). Royal Society of Chemistry; 2019. .
- [62] Mendiara T, Abad A, de Diego LF, García-Labiano F, Gayán P, Adánez J. Biomass combustion in a CLC system using an iron ore as an oxygen carrier. *International Journal of Greenhouse Gas Control*. 2013;19:322 – 330.
- [63] Mendiara T, Gayán P, García-Labiano F, de Diego LF, Pérez-Astray A, Izquierdo MT, et al. Chemical Looping Combustion of Biomass: An Approach to BECCS. *Energy Procedia*. 2017;114(13th International Conference on Greenhouse Gas Control Technologies, GHGT-13, 14-18 November 2016, Lausanne, Switzerland):6021 – 6029.
- [64] Berdugo Vilches T, Lind F, Rydén M, Thunman H. Experience of more than 1000h of operation with oxygen carriers and solid biomass at large scale. *Applied Energy*. 2017;190:1174 – 1183.
- [65] Leion H, Mattisson T, Lyngfelt A. Solid fuels in chemical-looping combustion. *International Journal of Greenhouse Gas Control*. 2008;2:180 – 193.
- [66] Jeremiáš M, Pohořelý M, Svoboda K, Manovic V, Anthony EJ, Skobliá S, et al. Full Length Article: Gasification of biomass with CO₂ and H₂O mixtures in a catalytic fluidised bed. *Fuel*. 2017;210:605 – 610.
- [67] Li Y, Wang H, Li W, Li Z, Cai N. CO₂ Gasification of a Lignite Char in Microfluidized Bed Thermogravimetric Analysis for Chemical Looping Combustion and Chemical Looping with Oxygen Uncoupling. *Energy & Fuels*. 2019;33(1):449–459.

